Electronic Supplementary Material (ESI) for ChemComm.

Creation and stabilization of carbon dots in silica-confined compartments with high thermal stability

Huan-Huan Zhang, Chuan-De Wu*

Key Laboratory of Excited-State Material of Zhejiang Province and State Key Laboratory of Silicon Materials, Department of Chemistry, Zhejiang University, Hangzhou, 310027, P. R. China

E-mail address: cdwu@zju.edu.cn

Experimental Section

Materials and methods

Tetraethyl orthosiliane (TEOS), (3-aminopropyl)triethoxysilane (APTES), and citric acid (CA) were all purchased from Chemical Energy Co., Ltd. All reagents were used as received without further purification. The morphologies of solid materials were analyzed by high resolution transmission electron microscopy (HRTEM) on a JEM 2100F equipment and transmission electron microscope (TEM) on a Hitachi HT-7700 equipment. UV-visible diffuse reflection (UV-Vis DRS) spectra were obtained with a TU-1901 spectrophotometer equipped with an integrating sphere by using $BaSO_4$ as a reflectance standard. Photoluminescence (PL) measurements were performed on a Hitachi F4600 fluorescence spectrometer at room temperature. The fluorescence decay curves of CDs@SiO_2 composite were obtained by using an EPL laser (375 nm) as the excitation source and the single-photo counting detector (ID-100) to collect emitting light. X-ray photoelectron spectroscopy (XPS) was recorded on a Thermo Scientific K-Alpha spectroscopy with Al-Kα irradiation (1486.6 eV), and the binding energies were calibrated using the C1s peak at 284.8 eV. Fourier transform infrared spectrometer (FT-IR) spectra were performed from KBr pellets on a Nicolet iS10 spectrophotometer in the range of 500-4000 cm^{-1}. Thermogravimetric analysis (TGA) experiments were carried out on a Pyris 1 TGA (Perkin-Elmer), and the heating rate is of 10 ^oC/min under N_2 and air atmospheres. N_2 adsorption/desorption isotherms were performed on a Micromeritics ASAP 2460 surface area analyzer. The static water contact angels were carried out by using sessile method on a JY-82C system at room temperature.

Synthesis of CDs@SiO_2 composite

Citric acid (0.25 mmol) was dissolved in a mixture of deionized water (10 mL) and methanol (45 mL). Then, TEOS (22.5 mL) was drop-added to the mixture under vigorous stirring. APTES (0.25 mmol) was added under continuously stirring at room temperature, and reacted for 6 h. The obtained gel was subsequently dried and aged at 80 °C for 2 days. The resulted white solid was pyrolyzed at 400 °C under nitrogen atmosphere to obtain CDs@SiO_2. The synthetic procedure of CDs@SiO_2-xR was similar to that of CDs@SiO_2, except that different amount of citric acid was added (xR represents the molar ratio of TEOS and CA).

Synthesis of unprotected CDs

5.0 mmol of CA and 5 mmol of APTES were dissolved in 25 mL of H_2O, and stirred at room temperature for 2 h. The mixture was transferred into a 50 mL teflon-lined stainless-steel autoclave, heated to 200 °C, and kept at this temperature for 12 h. After cooling to room temperature, the resulted solid was collected by filtration, washed with H_2O and EtOH, and finally dried in vacuum at 50 °C overnight to obtain unprotected CDs.[S1]

Figures

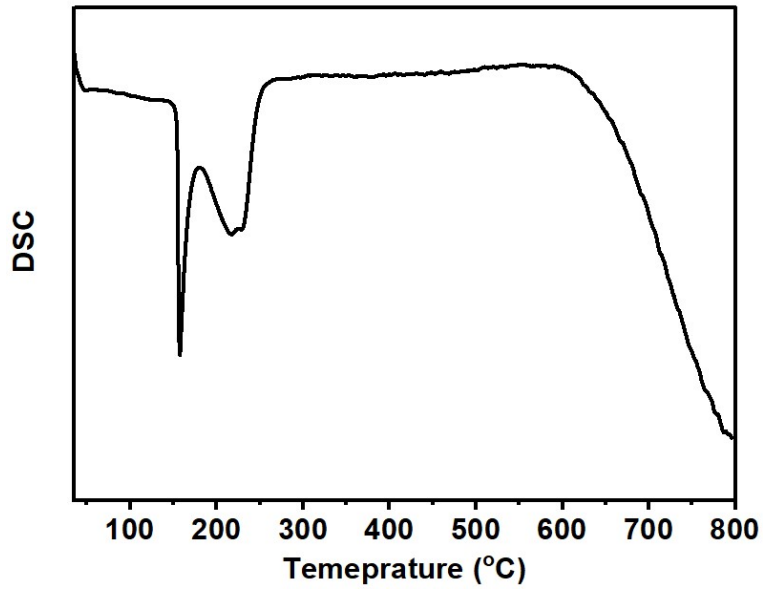

Fig. S1 DSC curve of citric acid under nitrogen atmosphere.

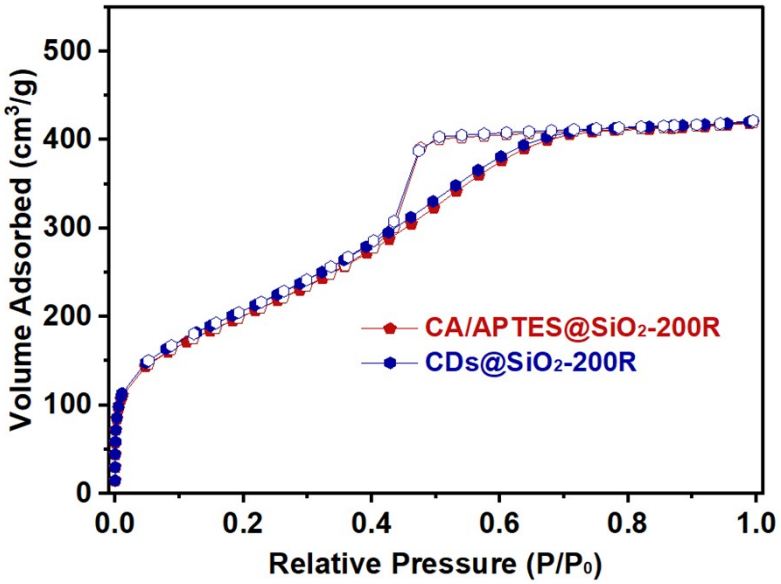

Fig. S2 N_2 sorption isotherms of CA/APTES@SiO_2-200R and CDs@SiO_2-200R.

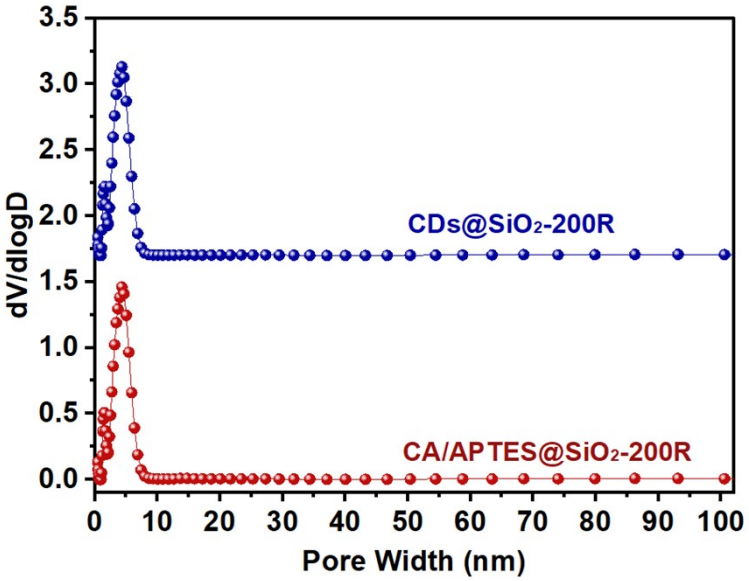

Fig. S3 Pore size distributions of CA/APTES@SiO_2-200R and CDs@SiO_2-200R.

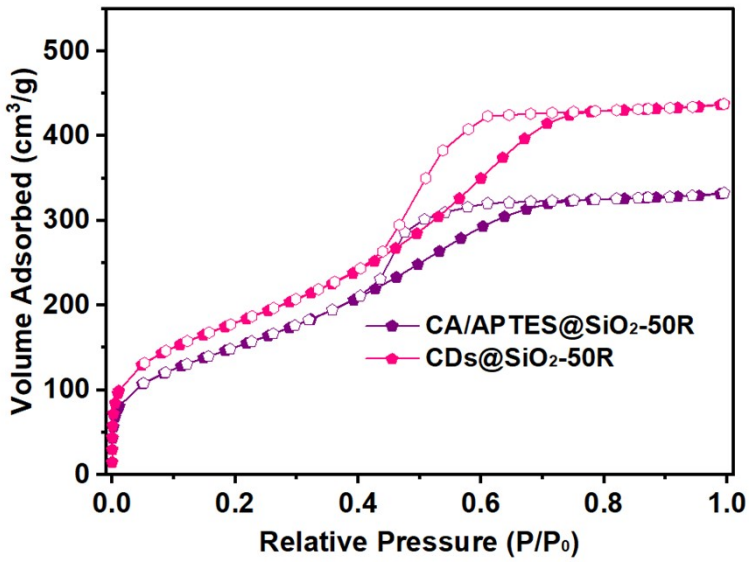

Fig. S4 N_2 sorption isotherms of CA/APTES@SiO_2-50R and CDs@SiO_2-50R.

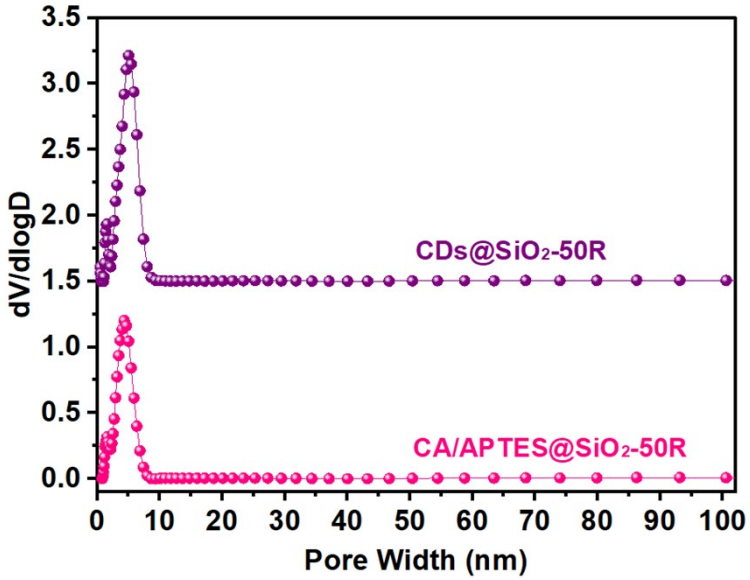

Fig. S5 Pore size distributions of CA/APTES@SiO_2-50R and CDs@SiO_2-50R.

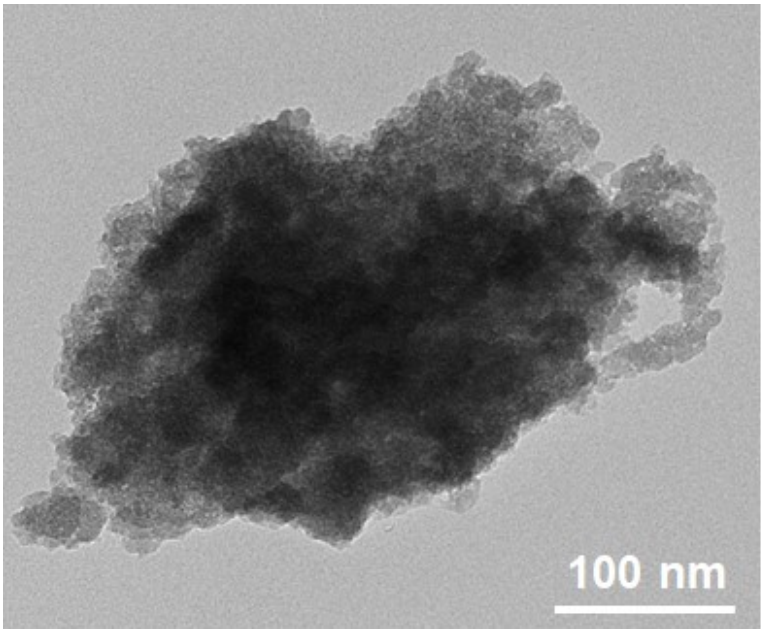

Fig. S6 TEM image of CDs@SiO_2 annealed at 100 °C.

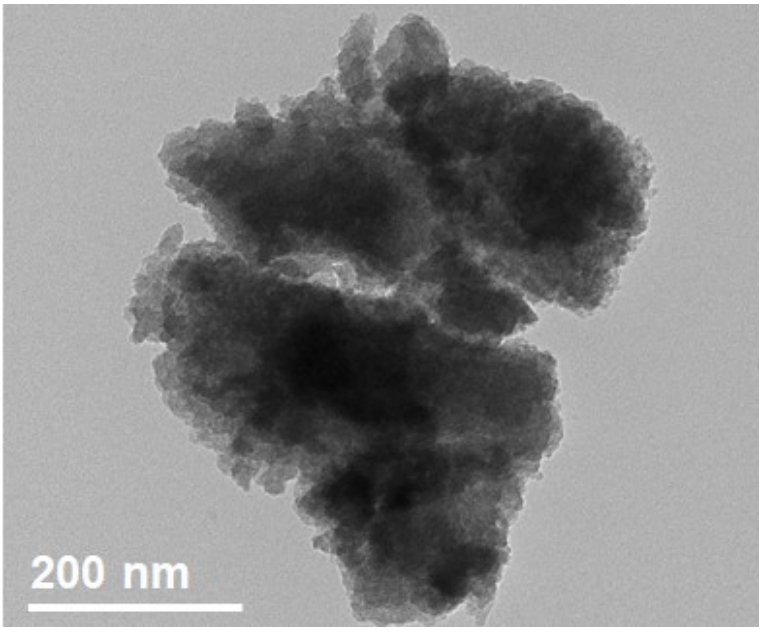

Fig. S7 TEM image of CDs@SiO_2 annealed at 200 °C.

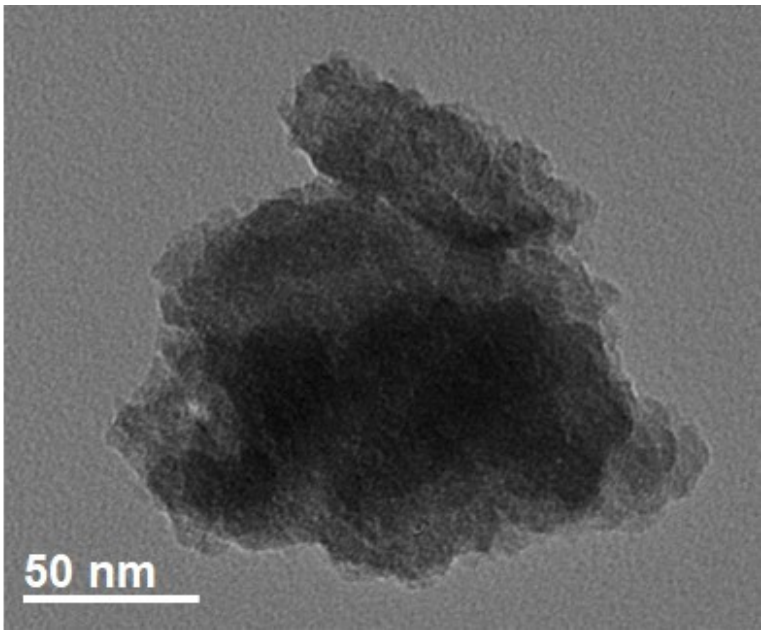

Fig. S8 TEM image of CDs@SiO_2 annealed at 300 °C.

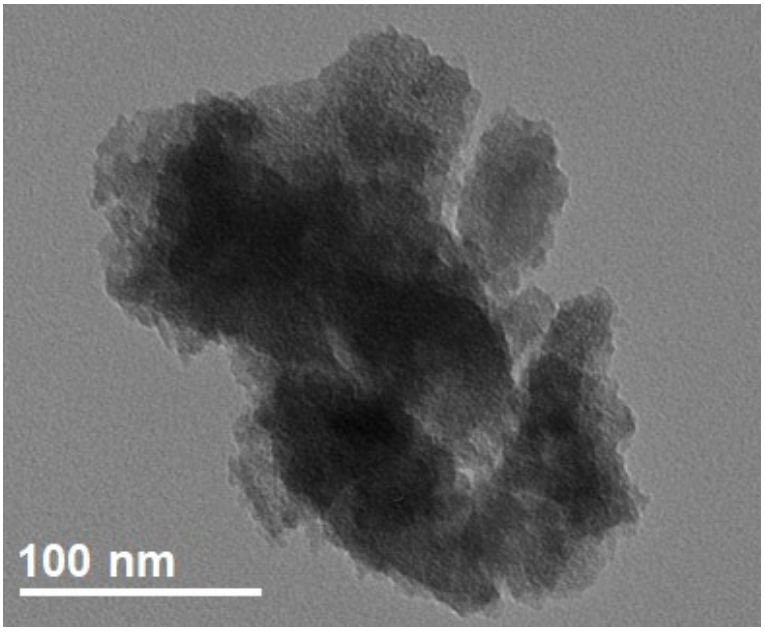

Fig. S9 TEM image of CDs@SiO_2 annealed at 400 °C.

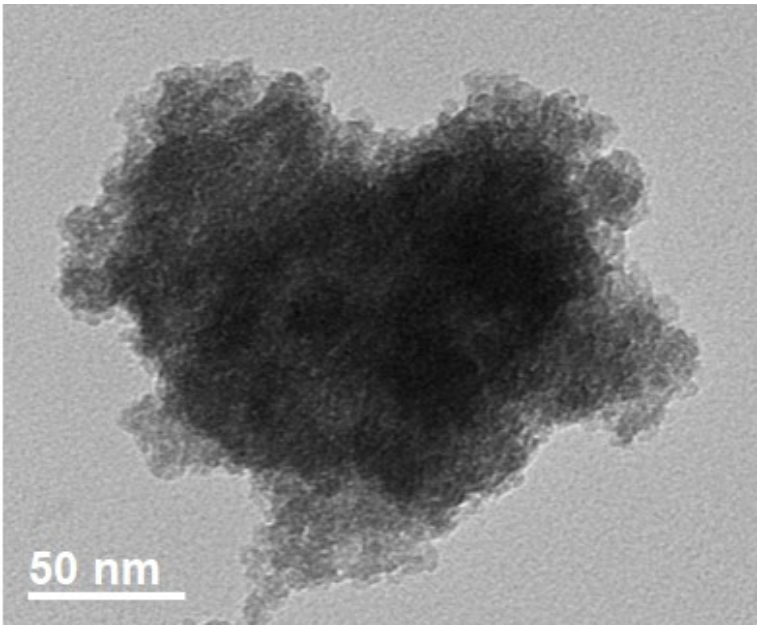

Fig. S10 TEM image of CDs@SiO_2 annealed at 500 °C.

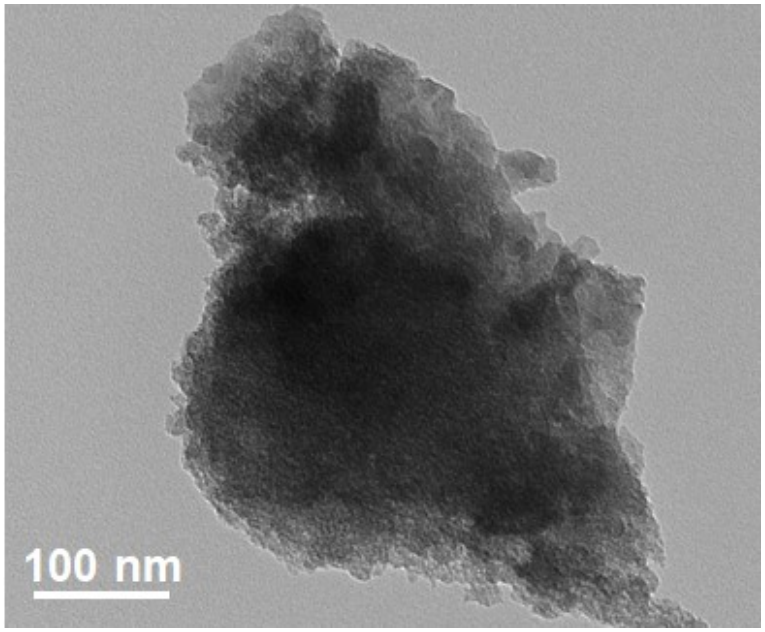

Fig. S11 TEM image of CDs@SiO_2 annealed at 600 °C.

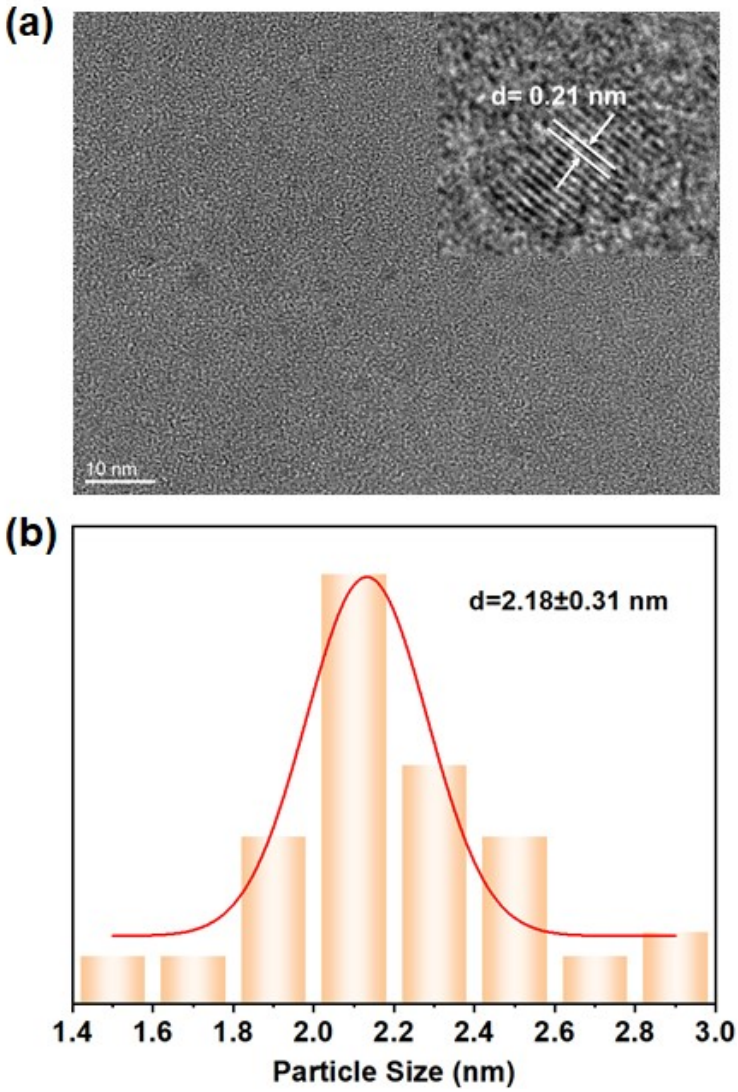

Fig. S12 (a) HRTEM images (inset: lattice spacing) and (b) histograms of particle size distribution of CDs released from CDs@SiO_2 annealed at 200 °C.

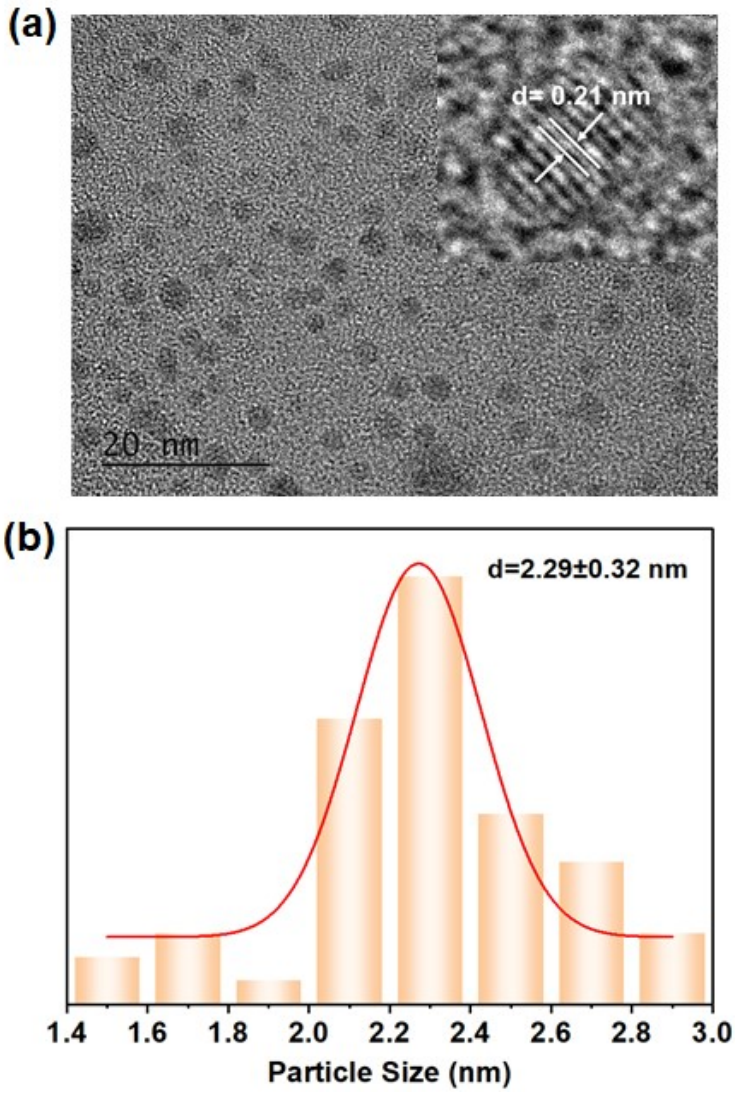

Fig. S13 (a) HRTEM images (inset: lattice spacing) and (b) histograms of particle size distribution of CDs released from CDs@SiO_2 annealed at 300 °C.

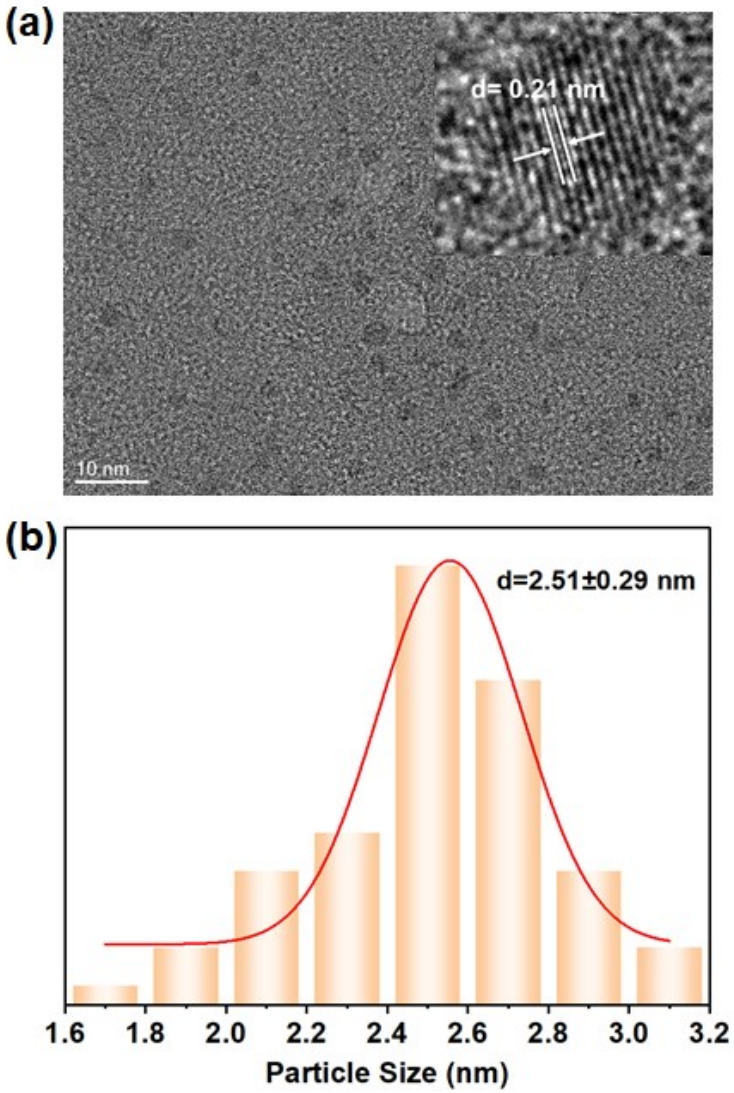

Fig. S14 (a) HRTEM images (inset: lattice spacing) and (b) histograms of particle size distribution of CDs released from CDs@SiO_2 annealed at 500 °C.

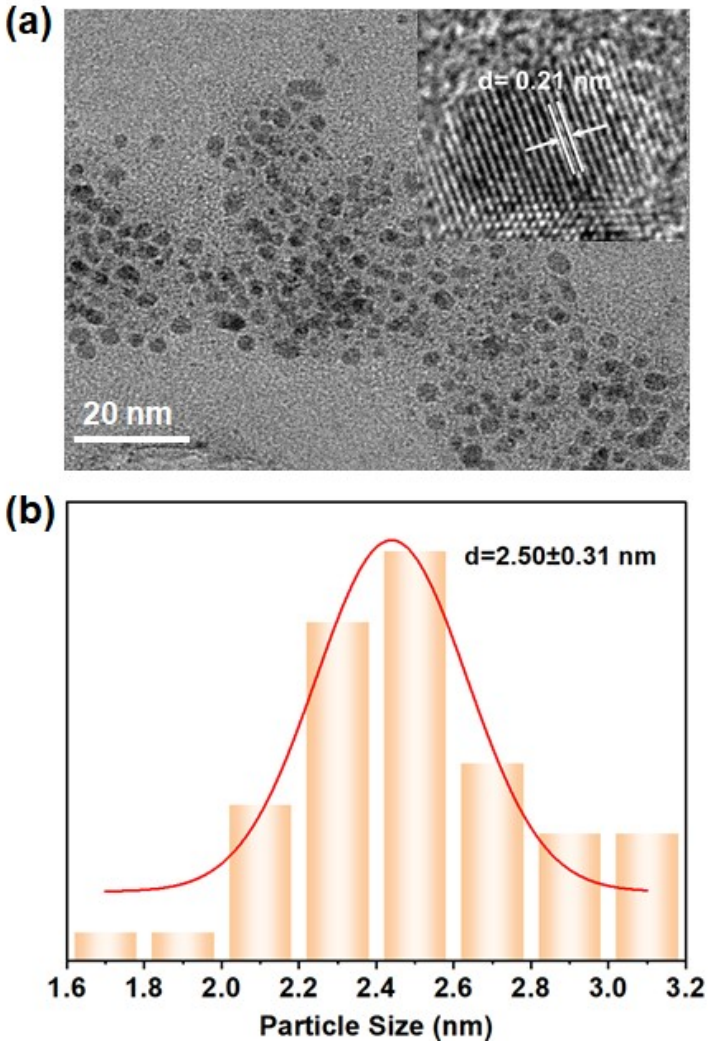

Fig. S15 (a) HRTEM images (inset: lattice spacing) and (b) histograms of particle size distribution of CDs released from CDs@SiO_2 annealed at 600 °C.

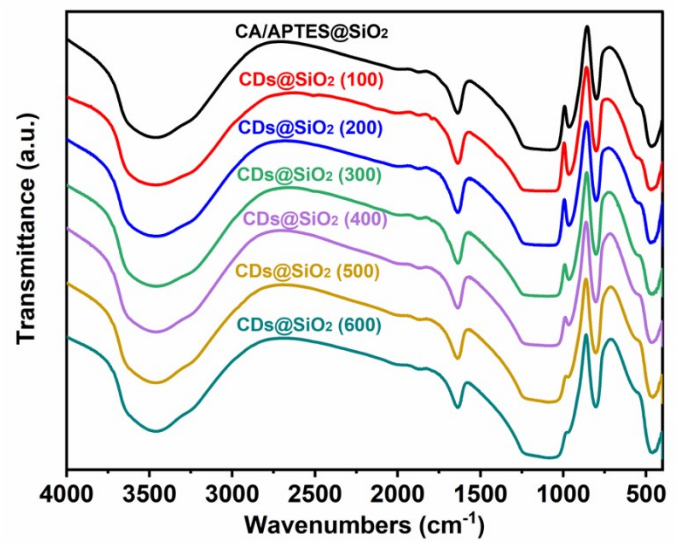

Fig. S16 FT-IR spectra of CA/APTES@SiO_2 and the annealed samples at different temperatures (the number in the parenthesis represents the annealing temperature).

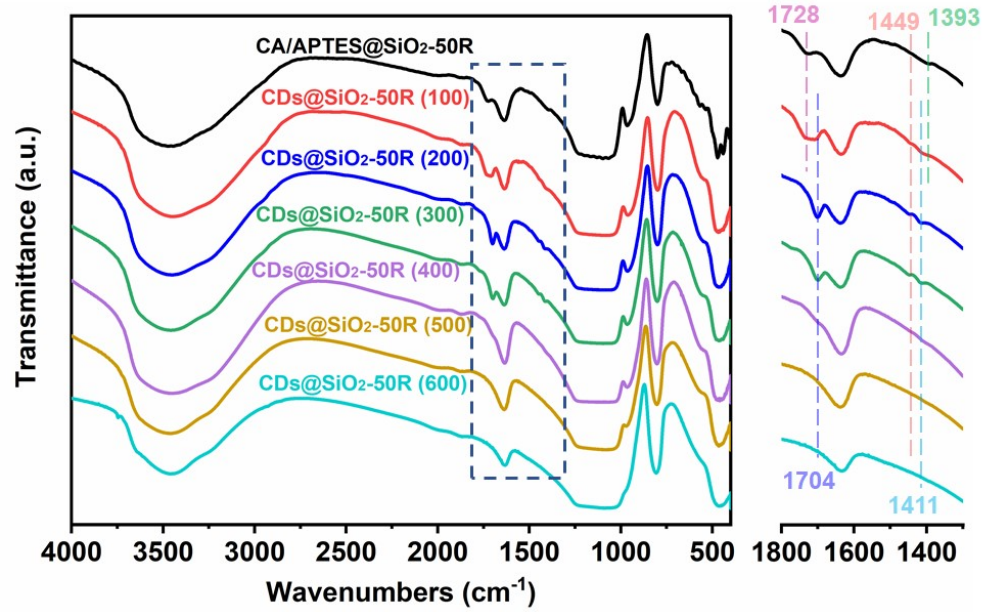

Fig. S17 FT-IR spectra of CA/APTES@SiO_2-50R and the annealed samples at different temperatures (the number in the parenthesis represents the annealing temperature).

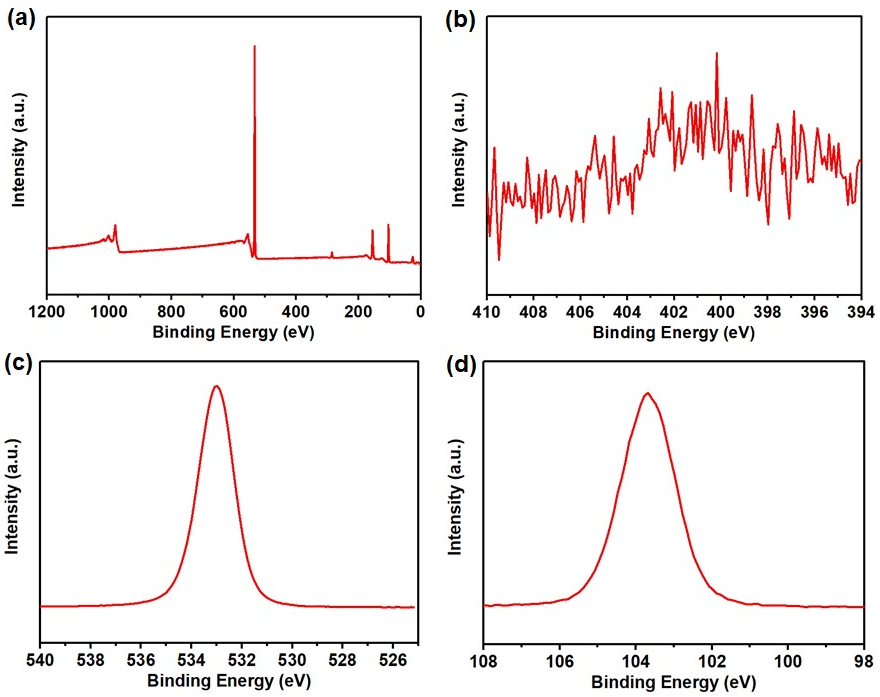

Fig. S18 The XPS spectra of survey (a), N 1s (b), O 1s (c) and Si 2p (d) for CDs@SiO_2 annealed at 100 °C.

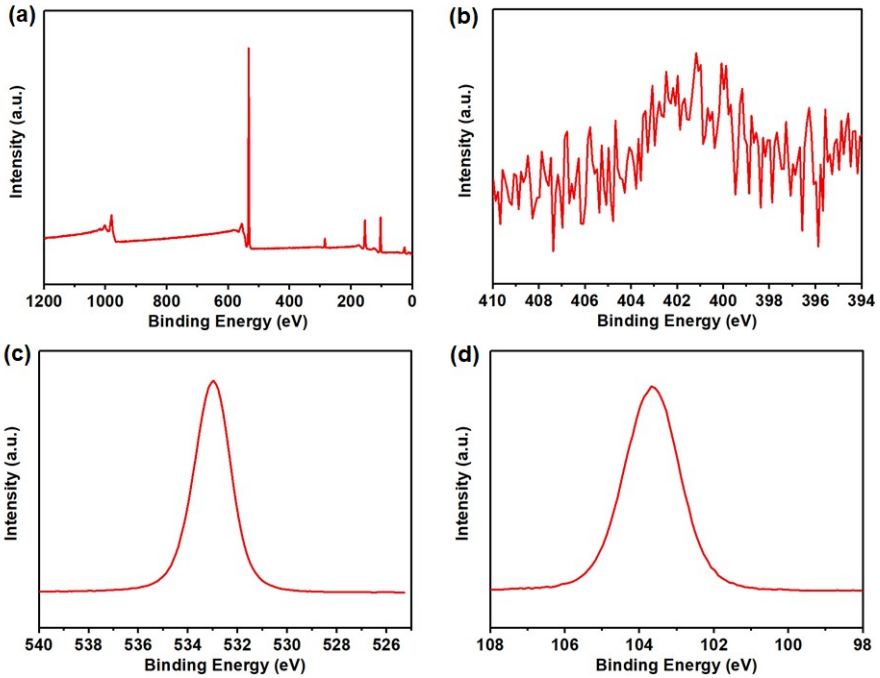

Fig. S19 The XPS spectra of survey (a), N 1s (b), O 1s (c) and Si 2p (d) for CDs@SiO_2 annealed at 200 °C.

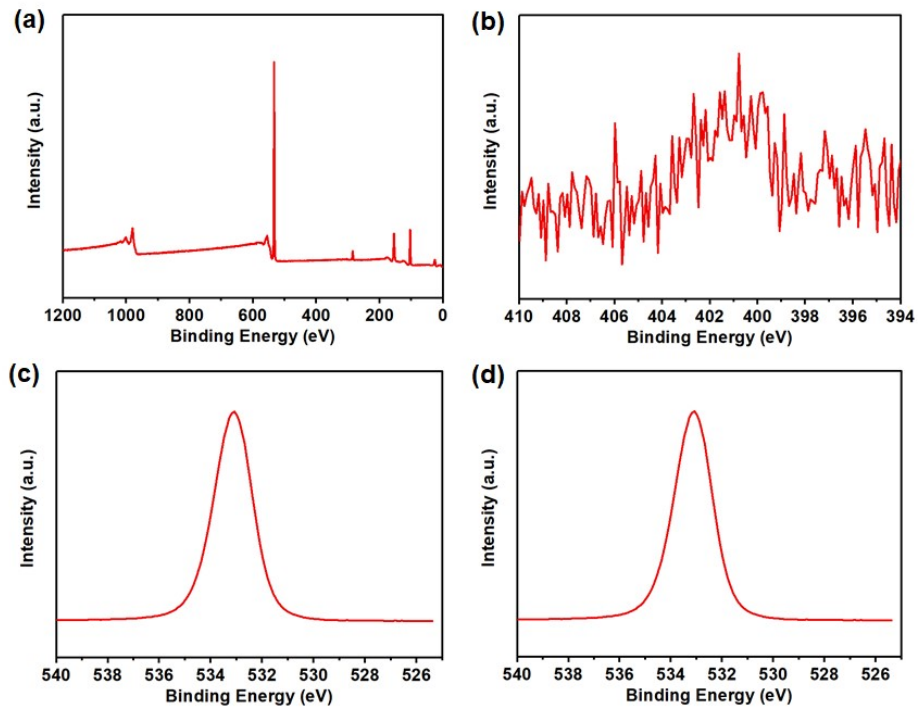

Fig. S20 The XPS spectra of survey (a), N 1s (b), O 1s (c) and Si 2p (d) for CDs@SiO_2 annealed at 300 °C.

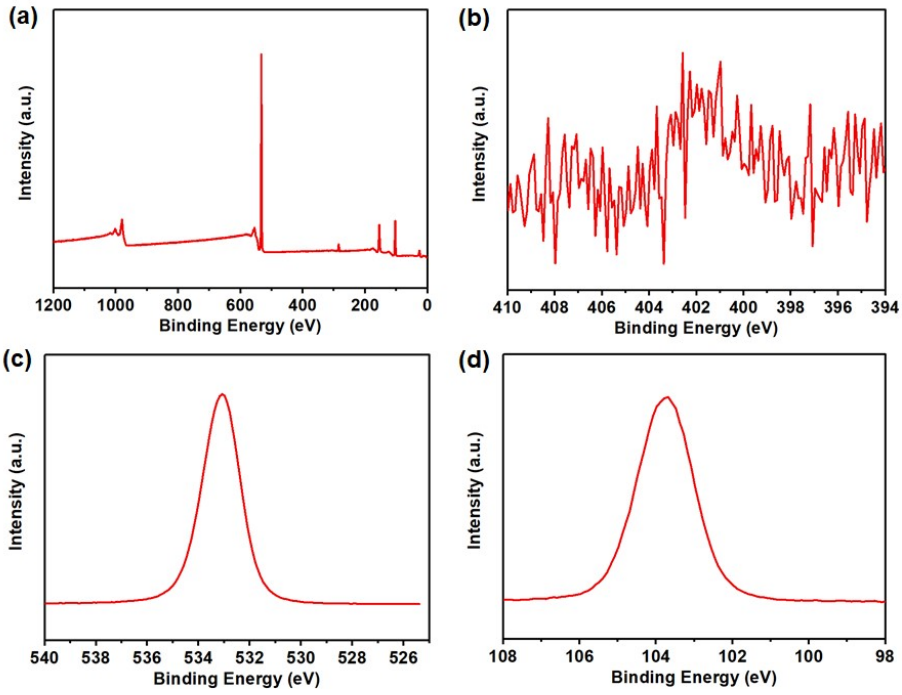

Fig. S21 The XPS spectra of survey (a), N 1s (b), O 1s (c) and Si 2p (d) for CDs@SiO_2 annealed at 400 °C.

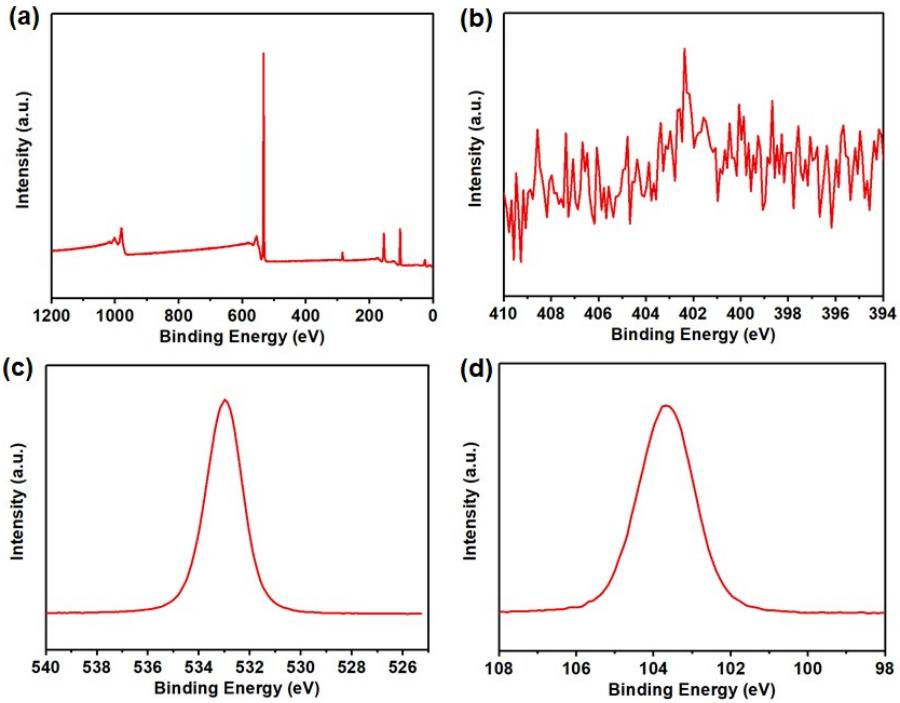

Fig. S22 The XPS spectra of survey (a), N 1s (b), O 1s (c) and Si 2p (d) for CDs@SiO_2 annealed at 500 °C.

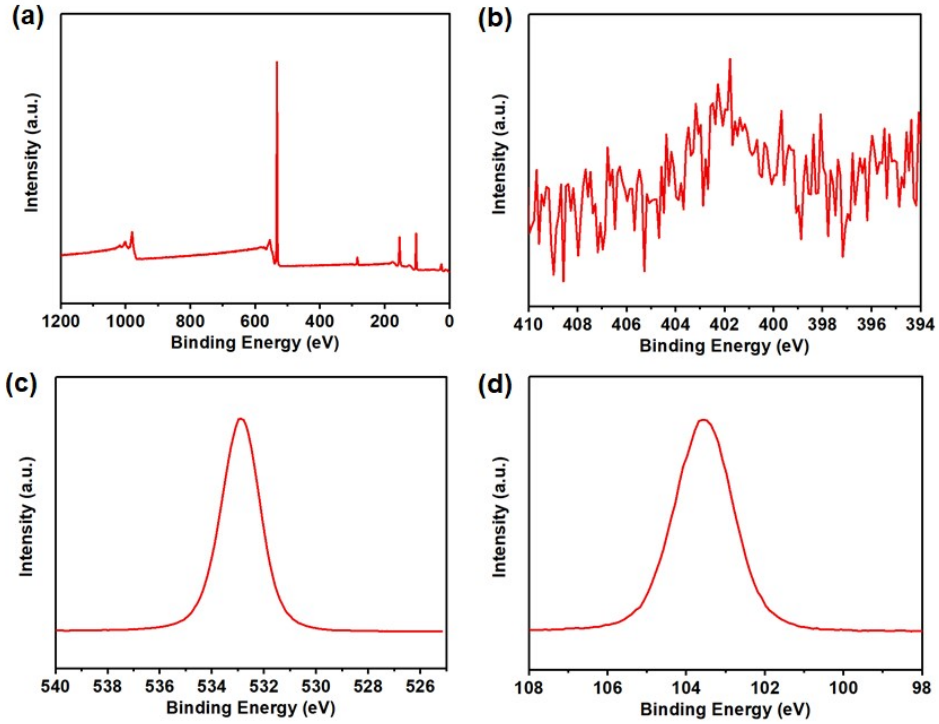

Fig. S23 The XPS spectra of survey (a), N 1s (b), O 1s (c) and Si 2p (d) for CDs@SiO_2 annealed at 600 °C.

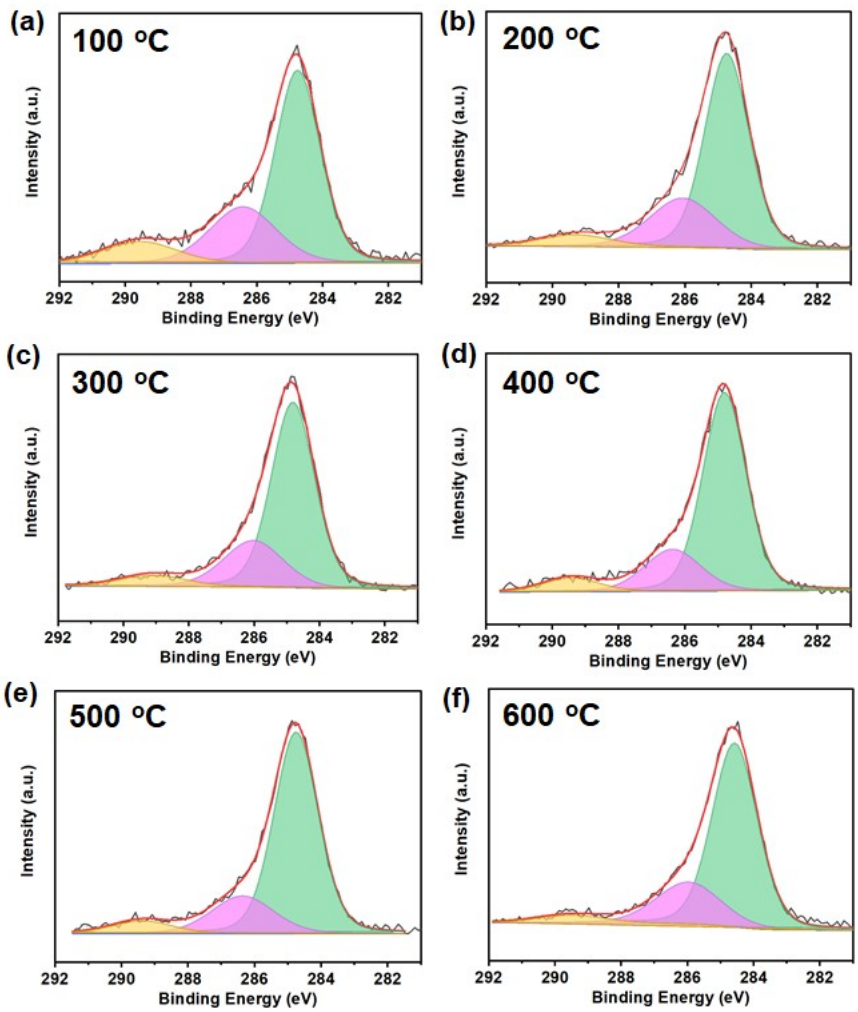

Fig. S24 The C 1s XPS spectra of the annealed products of CA/APTES@SiO_2 at different temperatures.

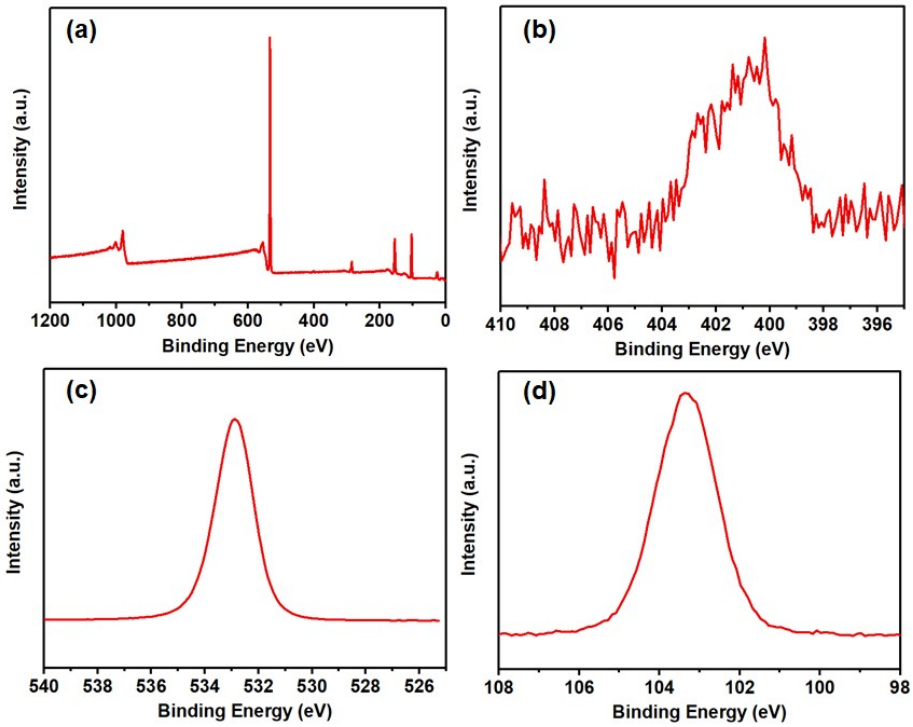

Fig. S25 The XPS spectra of survey (a), N 1s (b), O 1s (c) and Si 2p (d) for CDs@SiO_2-50R annealed at 100 °C.

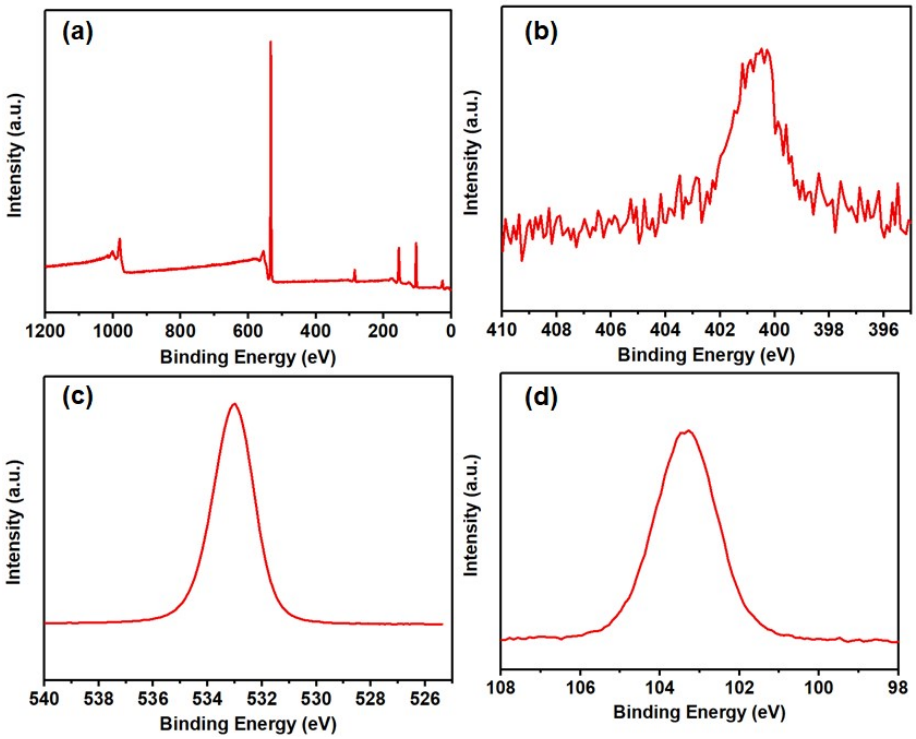

Fig. S26 The XPS spectra of survey (a), N 1s (b), O 1s (c) and Si 2p (d) for CDs@SiO_2-50R annealed at 200 °C.

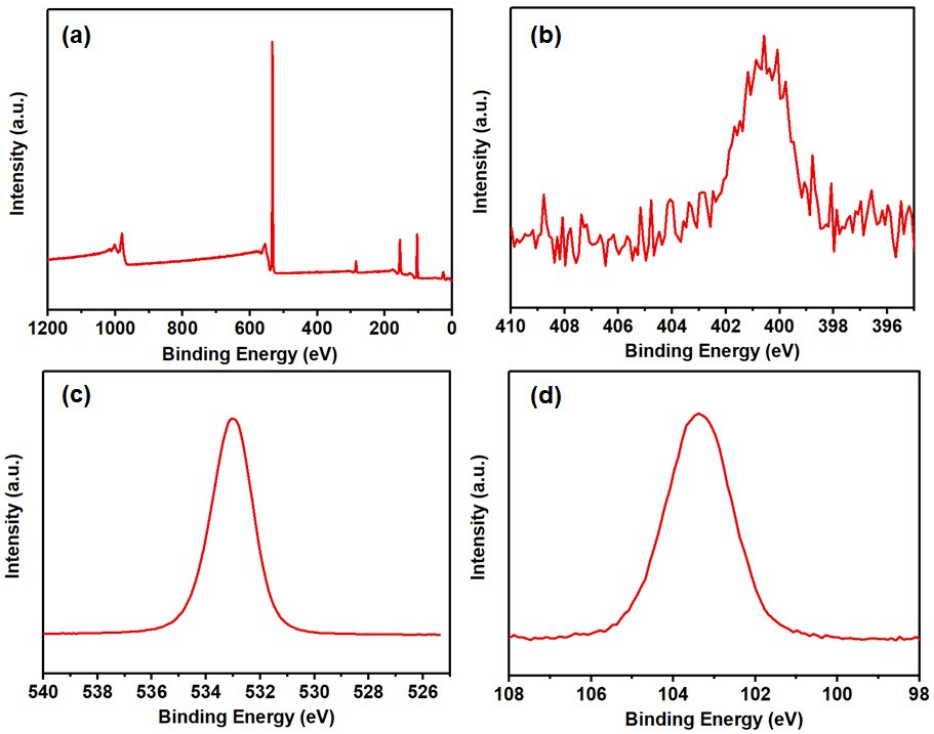

Fig. S27 The XPS spectra of survey (a), N 1s (b), O 1s (c) and Si 2p (d) for CDs@SiO_2-50R annealed at 300 °C.

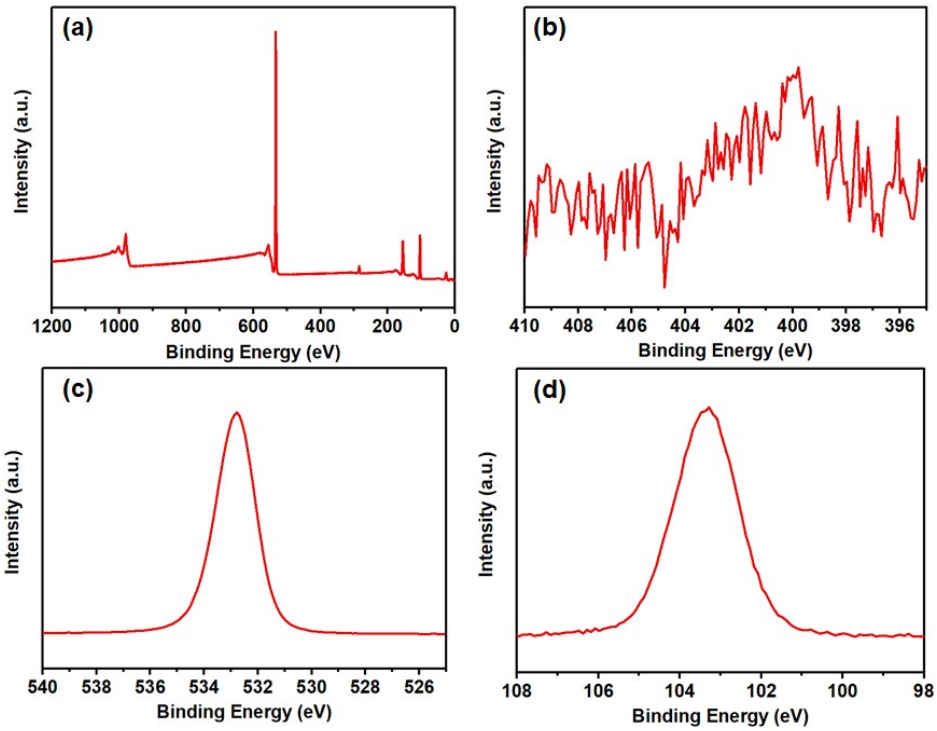

Fig. S28 The XPS spectra of survey (a), N 1s (b), O 1s (c) and Si 2p (d) for CDs@SiO_2-50R annealed at 400 °C.

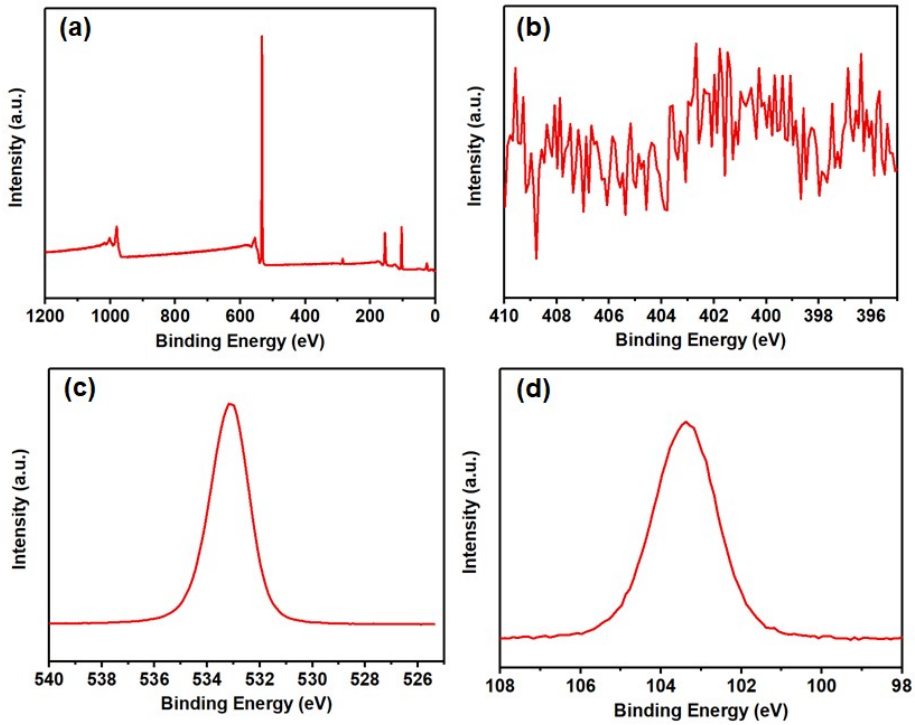

Fig. S29 The XPS spectra of survey (a), N 1s (b), O 1s (c) and Si 2p (d) for CDs@SiO_2-50R annealed at 500 °C.

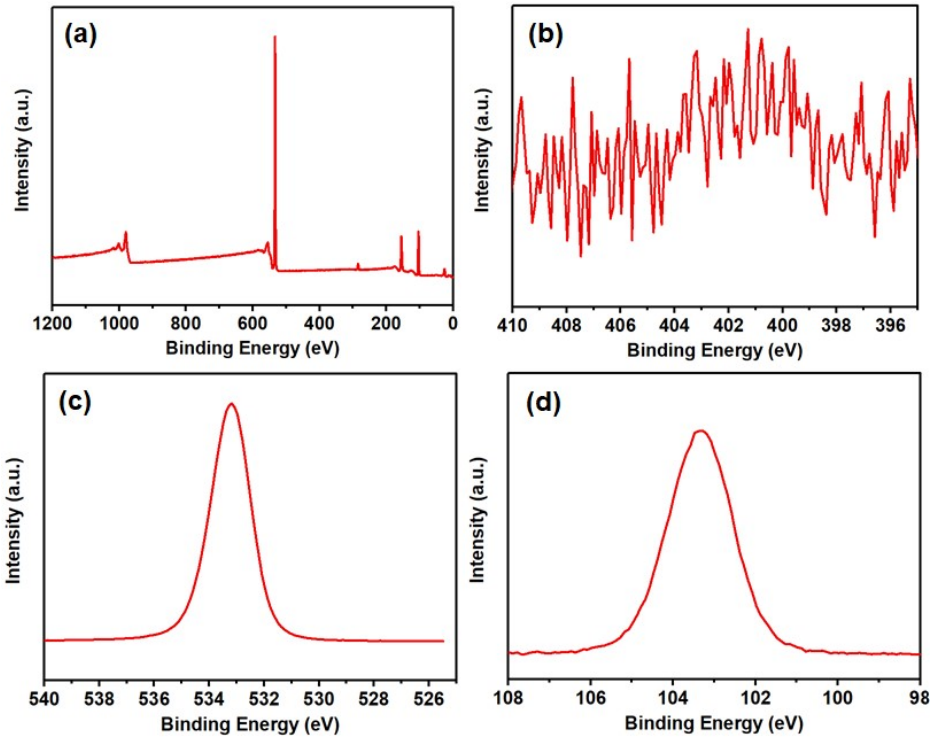

Fig. S30 The XPS spectra of survey (a), N 1s (b), O 1s (c) and Si 2p (d) for CDs@SiO_2-50R annealed at 600 °C.

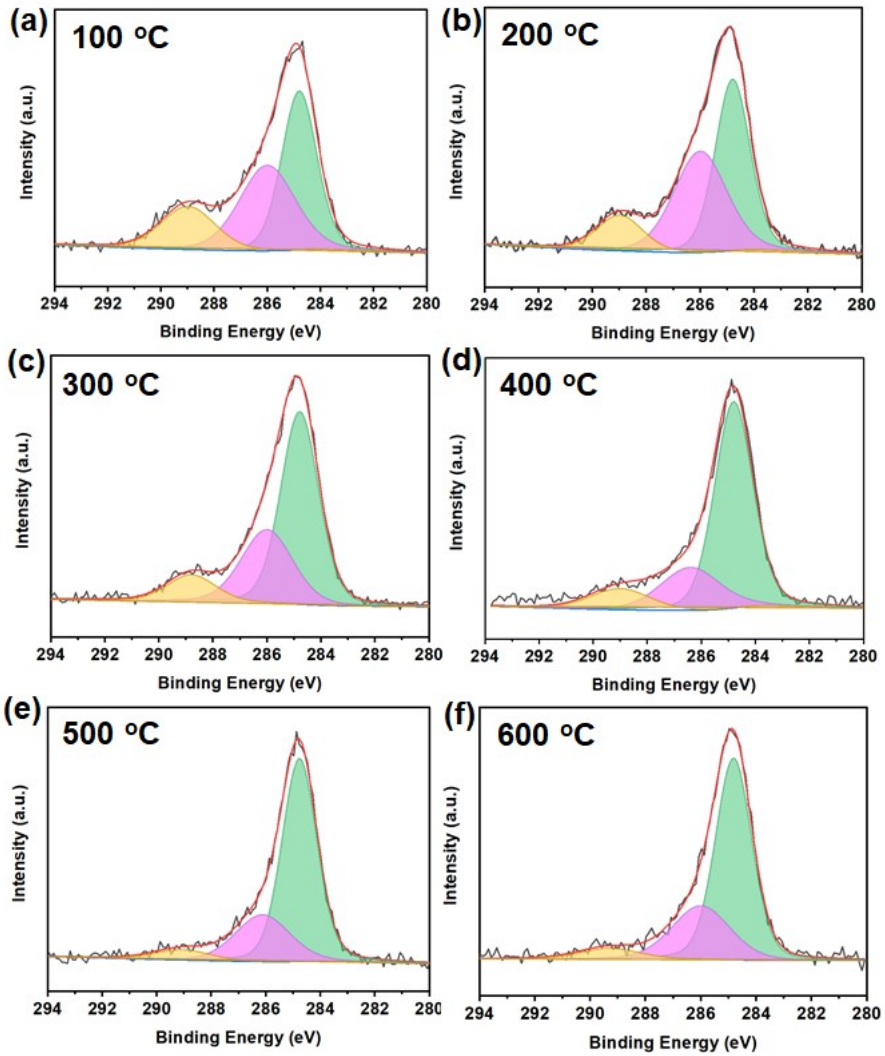

Fig. S31 The C1s XPS spectra of the annealed products of CA/APTES@SiO_2-50R at different temperatures.

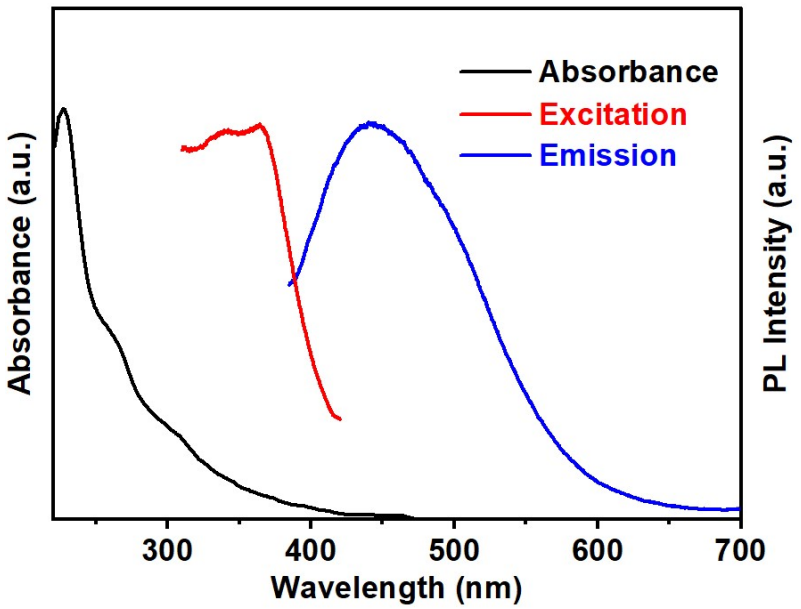

Fig. S32 UV-Vis DRS, PL excitation and emission spectra of CDs@SiO_2.

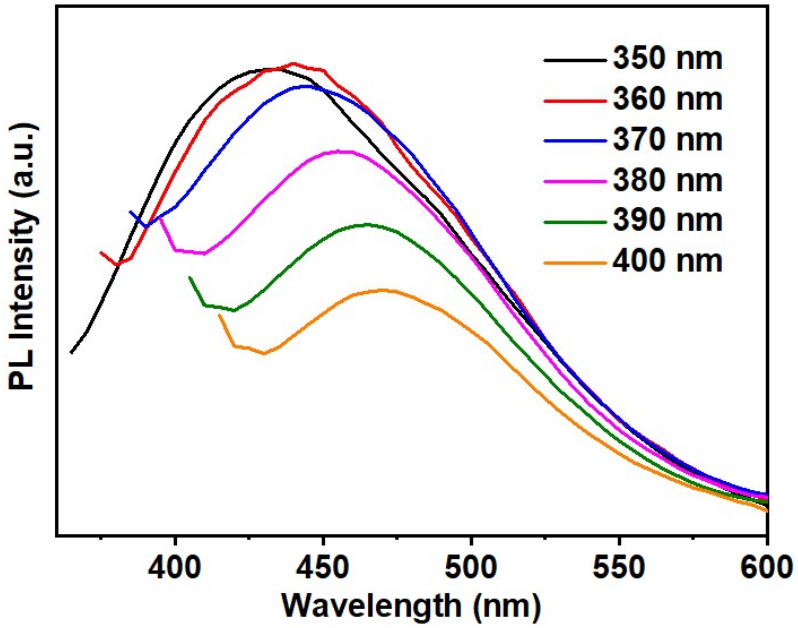

Fig. S33 PL emission spectra of CDs@SiO_2 under different excitation wavelengths.

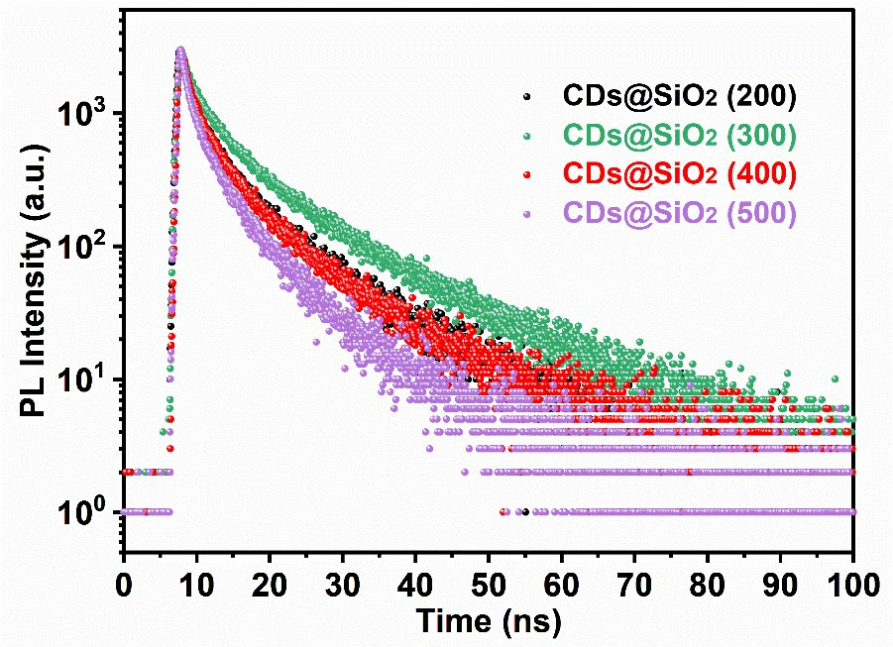

Fig. S34 Time-resolution PL of the annealed products for the CA/APTES@SiO_2 precursor at different temperatures with 375 nm excitation wavelength (the number in the parenthesis represents the annealing temperature).

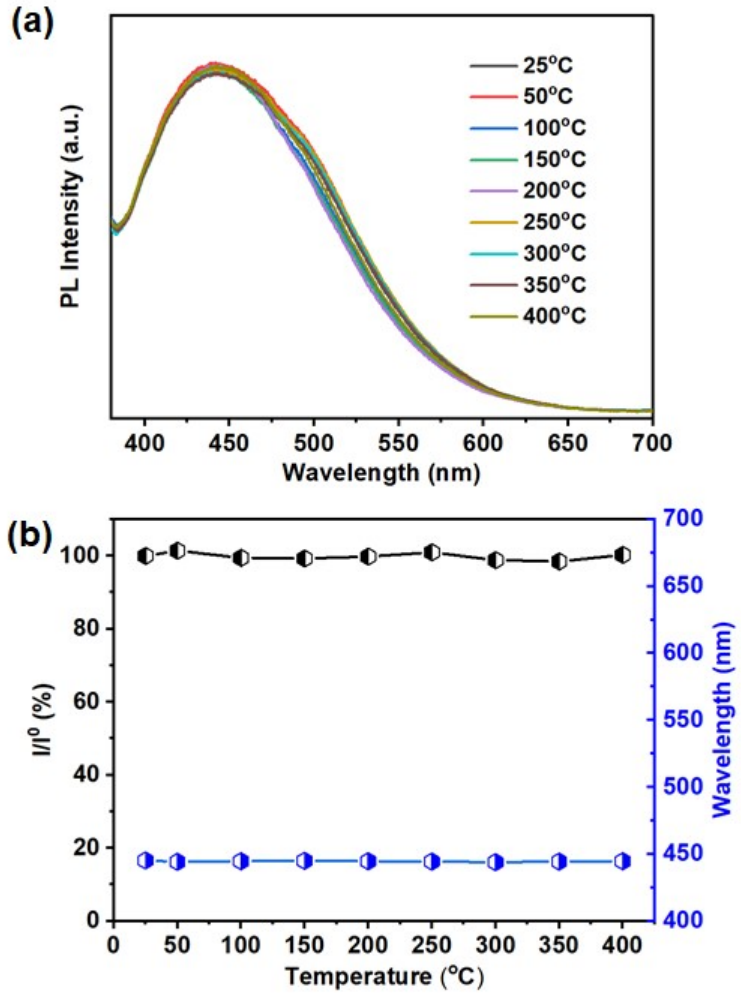

Fig. S35 (a) Solid state PL spectra of CDs@SiO_2 from 25 to 400 °C in nitrogen atmosphere. (b) Integrated PL intensity and emission peak position of CDs@SiO_2 versus temperature ranging from 25 to 400 °C in nitrogen atmosphere.

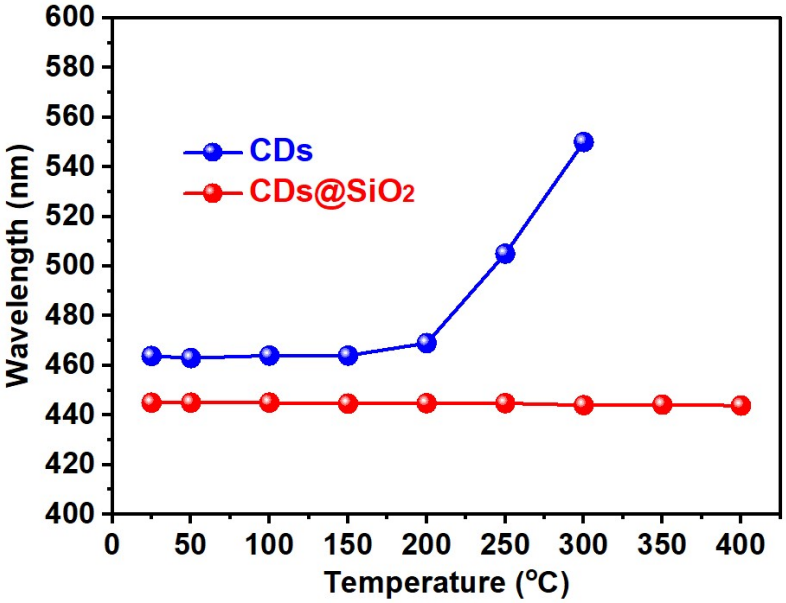

Fig. S36 Emission peak positions of CDs@SiO_2 and unprotected CDs versus temperature in air atmosphere.

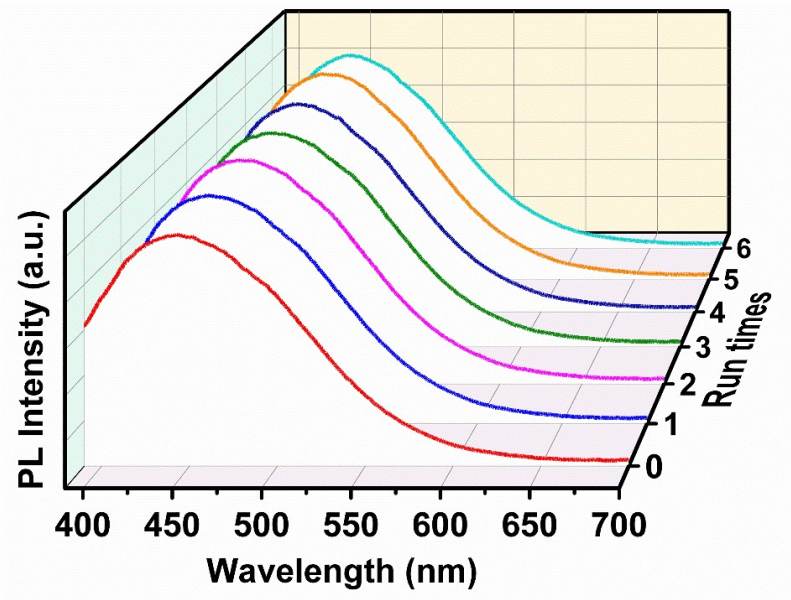

Fig. S37 PL spectra of CDs@SiO_2 heated at 350 °C for six cycles in air atmosphere.

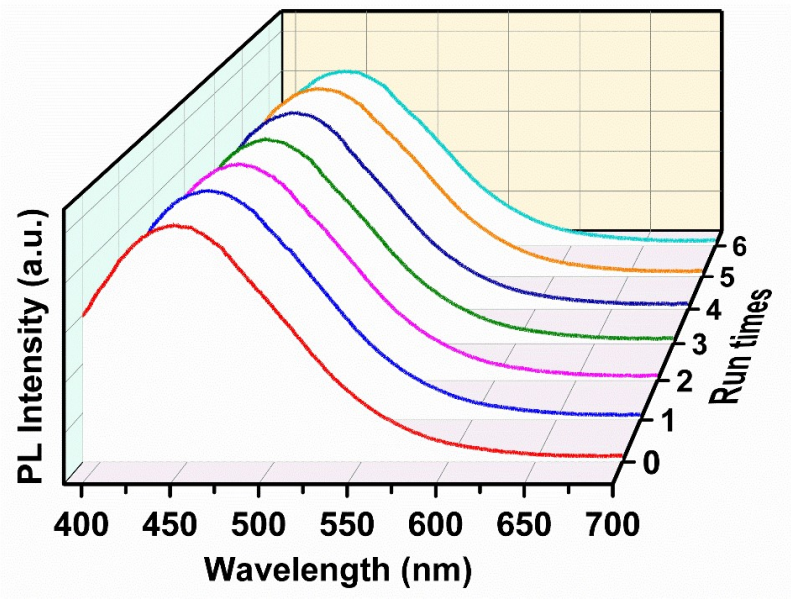

Fig. S38 PL spectra of CDs@SiO_2 heated at 400 °C for six cycles in air atmosphere.

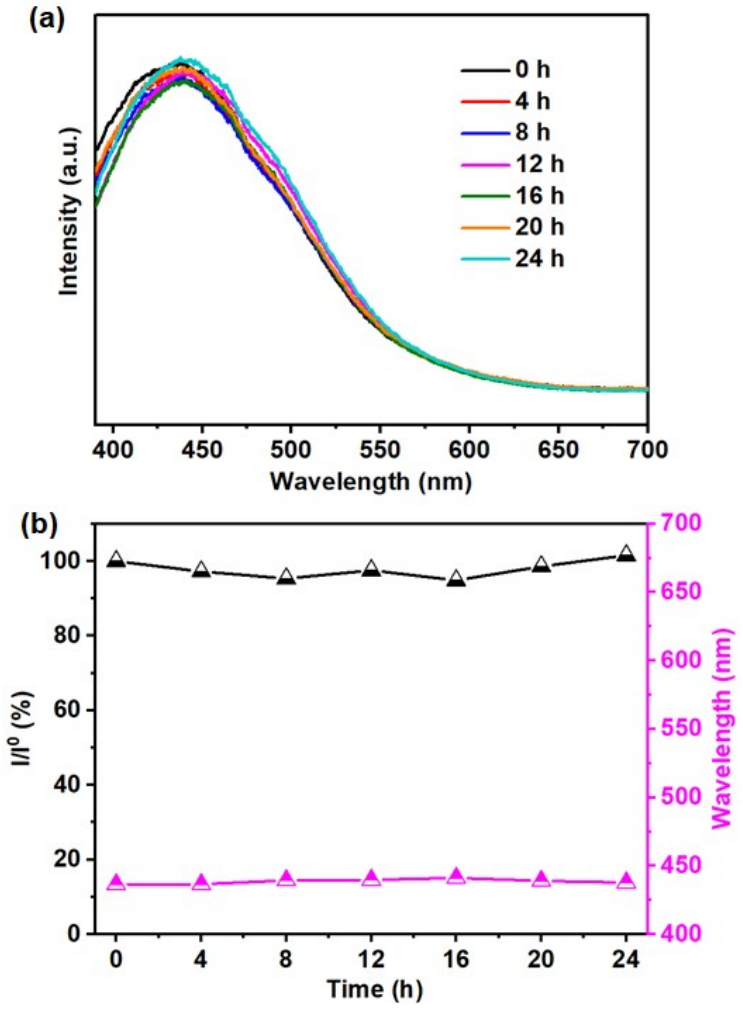

Fig. S39 (a) PL spectra of CDs@SiO_2 heated at 350 °C for 24 h in air atmosphere. (b) Integrated PL intensity and emission peak position of CDs@SiO_2 heated at 350 °C for 24 h in air atmosphere.

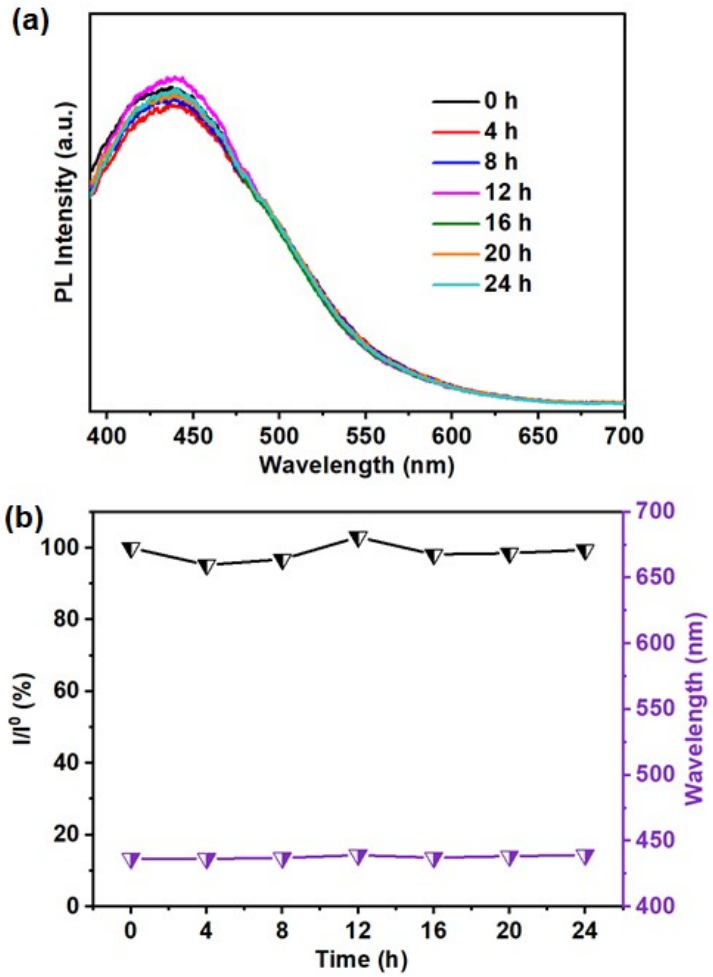

Fig. S40 (a) PL spectra of CDs@SiO_2 heated at 400 °C for 24 h in air atmosphere. (b) Integrated PL intensity and emission peak position of CDs@SiO_2 heated at 400 °C for different times in air atmosphere.

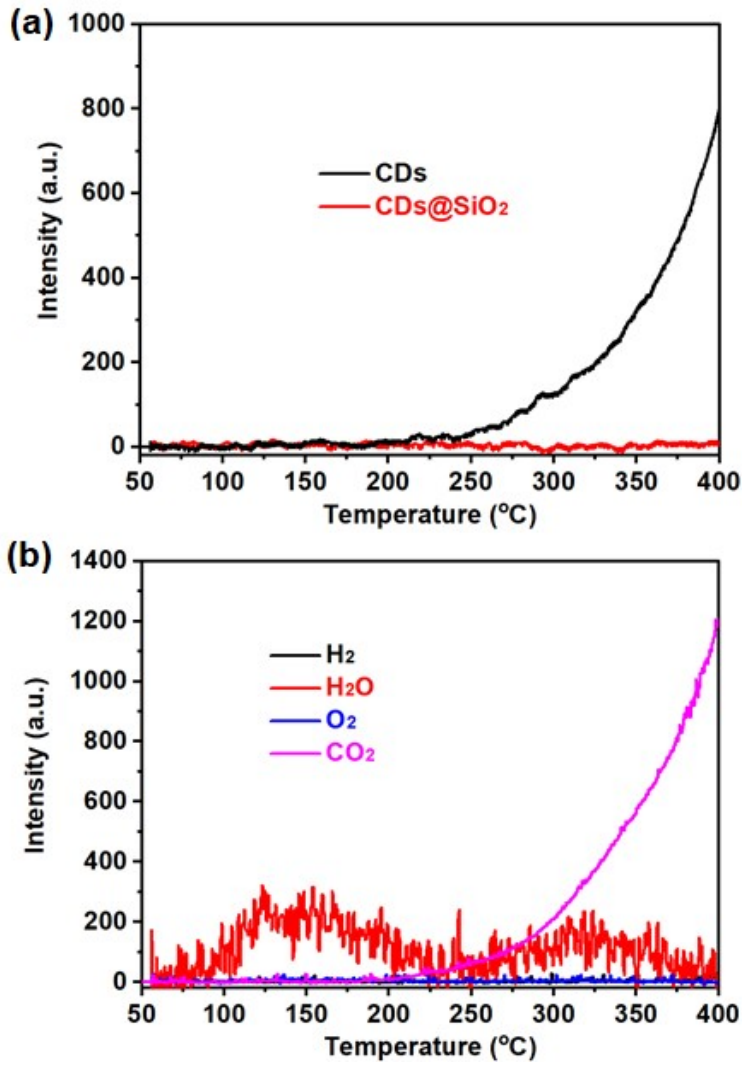

Fig. S41 (a) O_2-TPD spectra of CDs@SiO_2 and unprotected CDs. (b) Temperature-programmed desorption mass spectrometry of unprotected CDs.

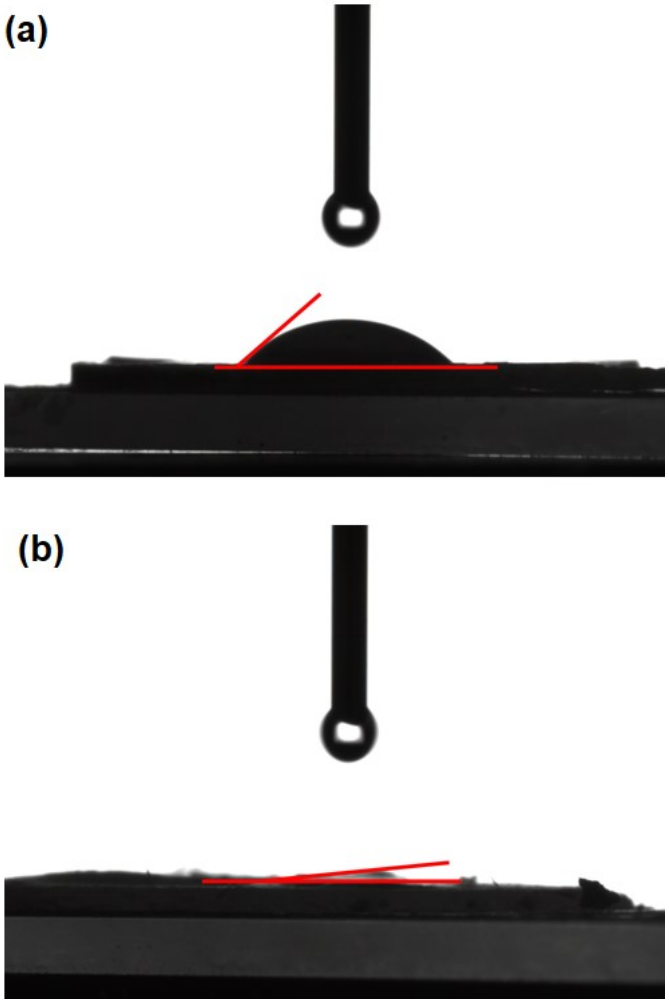

Fig. S42 Static water contact angles of (a) CDs@SiO_2 composite and (b) unprotected CDs (CDs@SiO_2 exhibits a water contact angel of 44°, and unprotected CDs presents a super-hydrophilic water contact angel of 5°).

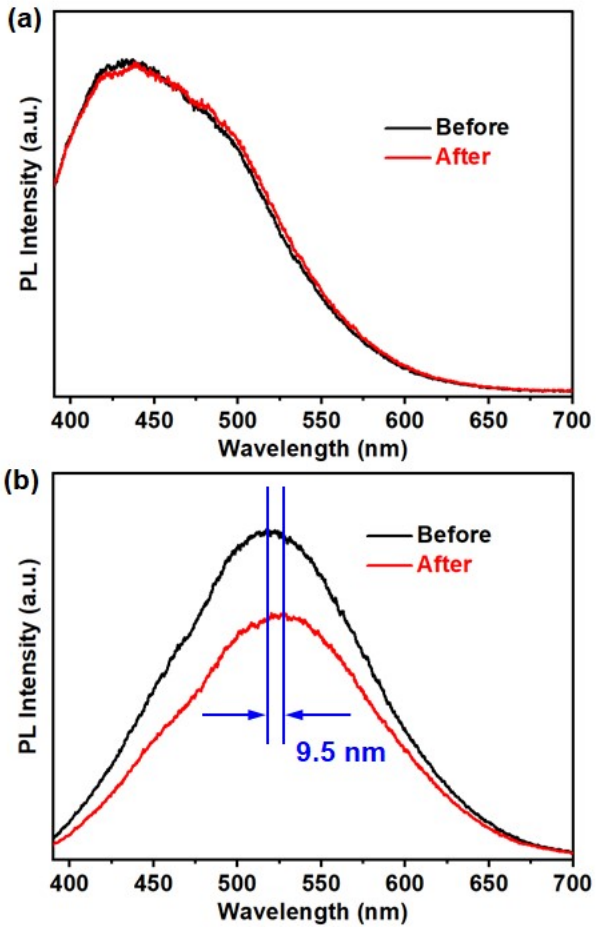

Fig. S43 (a) PL spectra of CDs@SiO_2 composite dispersed in water before and after heat treatment at 100 °C for one hour. (b) PL spectra of unprotected CDs dispersed in water before and after heat treatment at 100 °C for one hour.

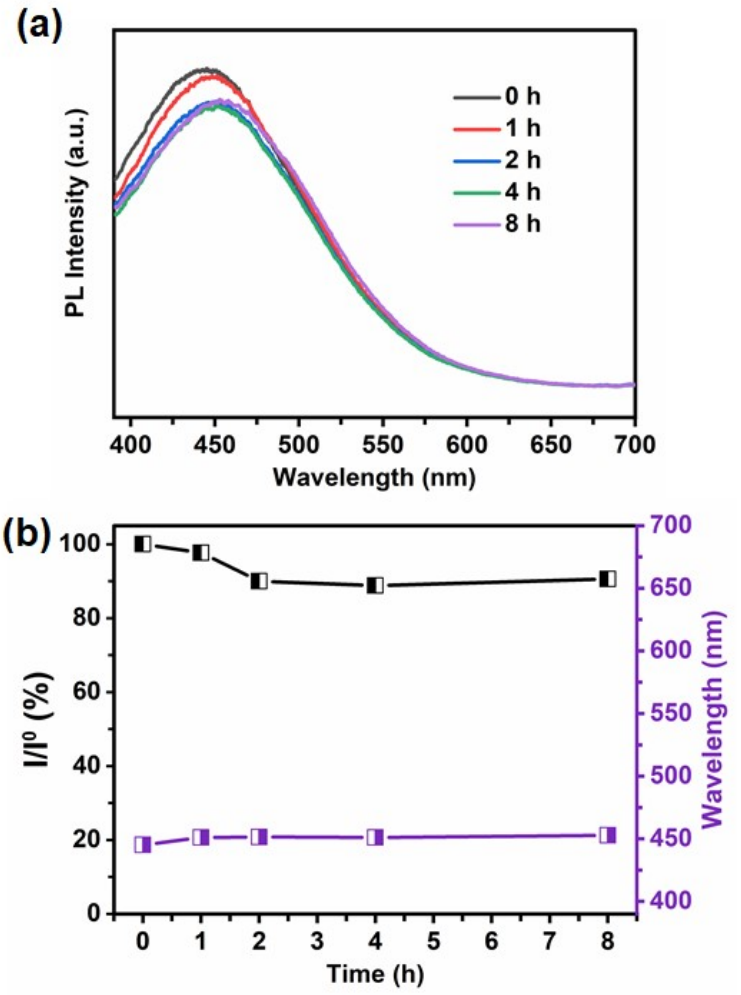

Fig. S44 (a) Photostability of CDs@SiO_2 under continuous irradiation with a 365 nm UV lamp for 8 h. (b) Integrated PL intensity and emission peak for CDs@SiO_2 at different times.

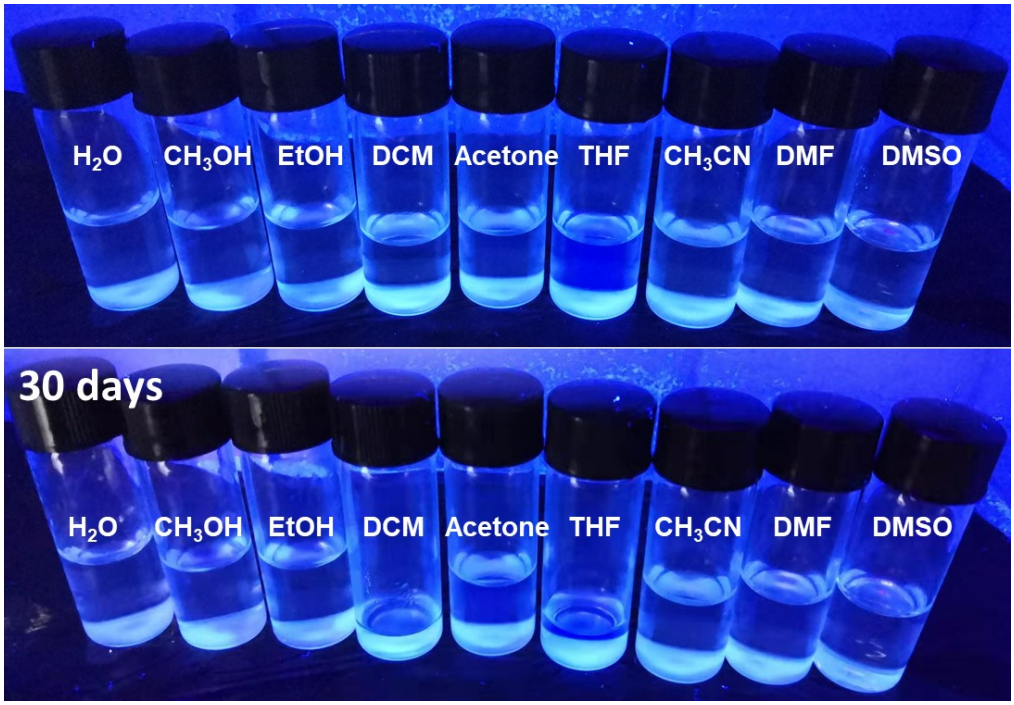

Fig. S45 Fluorescence images of CDs@SiO_2 in various solvents, taken under UV light irradiation.

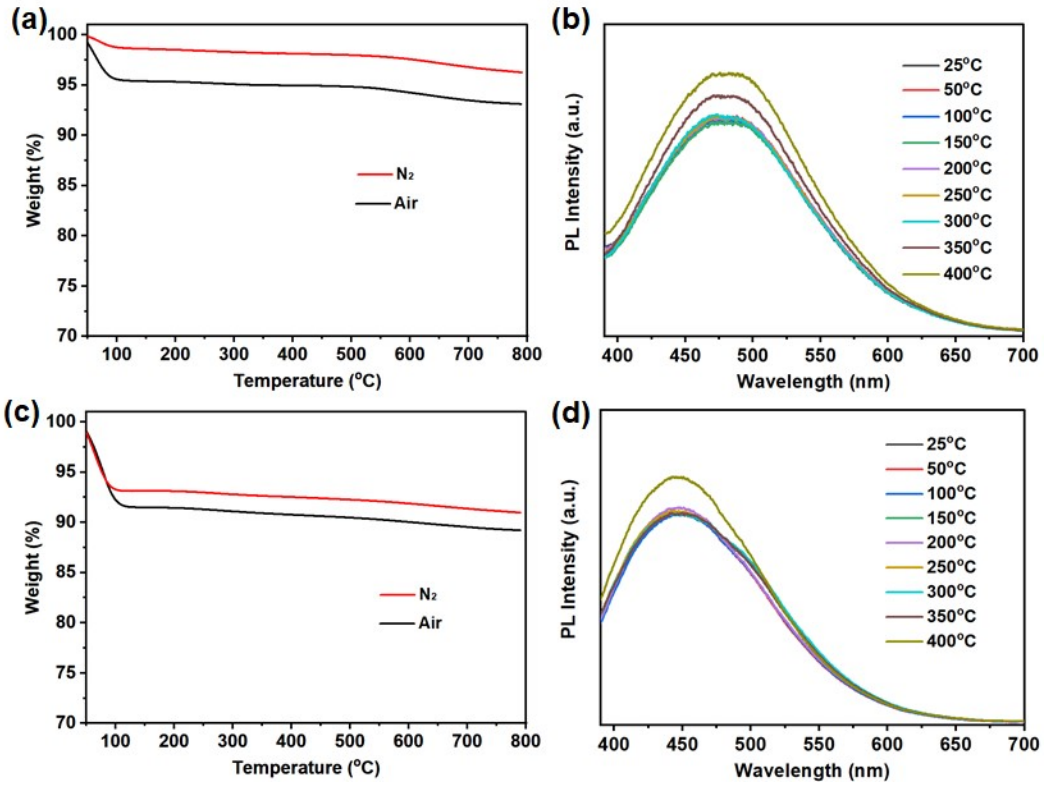

Fig. S46 (a) TGA curves of CDs@SiO_2-50R in N_2 and air atmospheres. (b) Solid state PL spectra of CDs@SiO_2-50R treated at different temperatures in air atmosphere. (c) TGA curves of CDs@SiO_2-200R in N_2 and air atmospheres. (d) Solid state PL spectra of CDs@SiO_2-200R treated at different temperatures in air atmosphere.

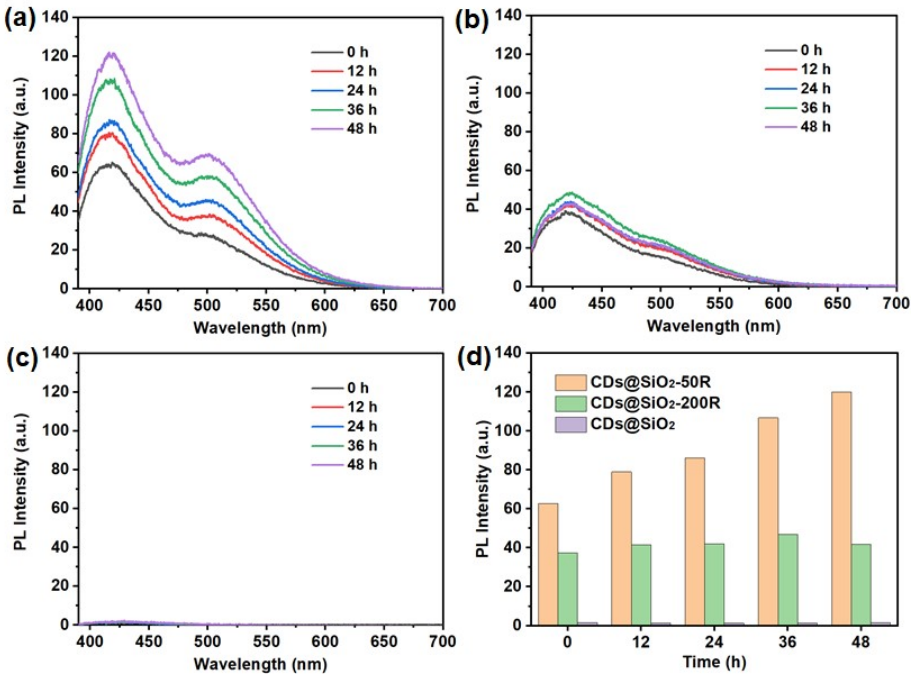

Fig. S47 PL spectra of the supernatants of (a) CDs@SiO_2-50R, (b) CDs@SiO_2-200R and (c) CDs@SiO_2 at different intervals. (d) The PL intensities of the supernatants of CDs@SiO_2-50R, CDs@SiO_2-200R and CDs@SiO_2 at different intervals.

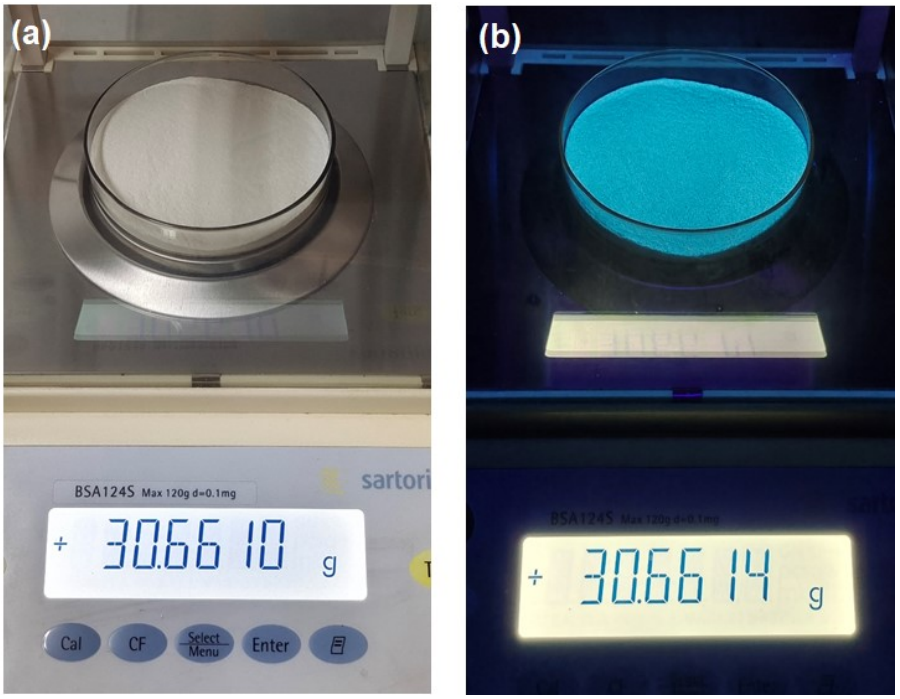

Fig. S48 Optical images of CDs@SiO_2 phosphors, taken under daylight (a) and UV light (b) irradiation.

Tables

Table S1 Textual properties of different materials

Sample	S_{BET} (m^2/g)	S_{micro} (m^2/g)	S_{ext} (m^2/g)	V_{pore} (cm^3/g)	V_{micro} (cm^3/g)
CA/APTES@SiO_2-50R	556	26	530	0.51	0.058
CDs@SiO_2-50R	607	204	403	0.67	0.29
CA/APTES@SiO_2-200R	738	117	621	0.65	0.12
CDs@SiO_2-200R	762	180	582	0.65	0.16
CA/APTES@SiO_2	740	151	588	0.78	0.20
CDs@SiO_2	740	171	569	0.77	0.21

Table S2 C 1s bonding states from XPS peak fitting for the annealed products of the CA/APTES@SiO_2 precursor at different temperatures

Sample	C-C/C=C (%)	C-O/C-N (%)	O-C=O (%)
CDs@SiO_2 (100)	61.74	26.72	11.54
CDs@SiO_2 (200)	68.08	25.49	6.43
CDs@SiO_2 (300)	69.95	23.85	6.20
CDs@SiO_2 (400)	73.21	20.12	6.68
CDs@SiO_2 (500)	74.14	19.44	6.42
CDs@SiO_2 (600)	72.15	23.39	4.46

Note: the number in the parenthesis represents the annealing temperature.

Table S3 C 1s bonding states from XPS peak fitting for the annealed products of the CA/APTES@SiO_2-50R precursor at different temperatures

Sample	C-C/C=C (%)	C-O/C-N (%)	O-C=O (%)
CDs@SiO_2-50R (100)	44.1	37.4	18.4
CDs@SiO_2-50R (200)	46.2	41.2	12.6
CDs@SiO_2-50R (300)	59.1	30.5	10.4
CDs@SiO_2-50R (400)	67.3	21.9	10.8
CDs@SiO_2-50R (500)	69.3	25.0	5.7
CDs@SiO_2-50R (600)	66.2	28.0	5.8

Note: the number in the parenthesis represents the annealing temperature.

Table S4 Life time of the annealed products of the CA/APTES@SiO_2 precursor at different temperatures

Sample	τ_1 (ns)	A_1 (%)	τ_2 (ns)	A_2 (%)	τ_3 (ns)	A_3 (%)	τ_{ave} (ns)
CDs@SiO_2 (200)	12.12	44.9	3.41	45.4	0.67	9.7	3.21
CDs@SiO_2 (300)	14.78	52.8	4.18	40.4	0.87	6.7	4.77
CDs@SiO_2 (400)	12.65	37.1	3.74	47.2	1.02	15.7	3.24
CDs@SiO_2 (500)	10.97	26.7	3.60	52.4	0.82	20.9	2.35

Note: the number in the parenthesis represents the annealing temperature.

Table S5 Summary of the thermal stability of solid-state CDs

Matrix	Treating temperature (^oC)	PL intensity retention (%)	Ref.
LDH	100	80	S2
Silica	100	95	S3
AlOOH	150	80	S4
$Mg(OH)_2$	150	89.6	S5
Al_2O_3	150	121.6	S6
$BaCl_2$	200	74.7	S7
$BaSO_4$	300	90	S8
SBA-15	400	60	S9
SiO_2	400	>99	This work

Note: LDH referred to layered double hydroxides.

References

S1 Y. Zhan, B. Shang, M. Chen and L. Wu, *Small*, 2019, **15**, 1901161.

S2 W. Liu, R. Liang and Y. Lin, *Nanoscale*, 2020, **23**, 7888-7894.

S3 M. Wang, Y. Han, Z. Guo, Z. Huang and W. Yang, *ACS Appl. Nano Mater.*, 2021, **4**, 13625-13632.

S4 J. Wu, S. Wang, S. Liu, S. Ma, G. Jing, Y. Hu, M. Wang, Z. Ye and X. Cheng, *J. Mater. Chem. C*, 2019, **7**, 14717-14724.

S5 Y. Xie, X. Geng, J. Gao, W. Shi, Z. Zhou, H. Wang, D. Zhang, B. Deng and R. Yu, *J. Alloys Compd.*, 2021, **873**, 159663.

S6 J. Chen, X. Zou, W. Li, H. Zhang, X. Zhang, M. S. Molokeev, Y. Liu and B. Lei, *Adv. Opt. Mater.*, 2022, **10**, 2200851.

S7 J. Liang, B. Yang, C.-Y. Zhong, J. Zhang, J. He, Y. Chen and Z.-Q. Liu, *Inorg. Chem. Front.*, 2020, **7**, 4845-4853.

S8 D. Zhou, Y. Zhai, S. Qu, D. Li, P. Jing, W. Ji, D. Shen and A. L. Rogach, *Small*, 2017, **13**, 1602055.

S9 Q. Chang, S. Yang, C. Xue, N. Li, Y. Wang, Y. Li, H. Wang, J. Yang and S. Hu, *Nanoscale*, 2019, **11**, 7247-7255.